

# Cu–Cr–O and Cu–Ce–O Regenerable Oxide Sorbents for Hot Gas Desulfurization

Zhijiang Li and Maria Flytzani-Stephanopoulos\*

Department of Chemical Engineering, Tufts University, Medford, Massachusetts 02155

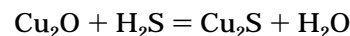
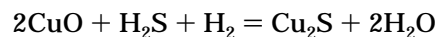
Binary Cu–Cr–O and Cu–Ce–O oxides were studied in this work as regenerable sorbents for high-temperature fuel gas desulfurization. CuO–Cr<sub>2</sub>O<sub>3</sub> and CuO–CeO<sub>2</sub> sorbents can remove H<sub>2</sub>S from simulated coal-derived fuel gas to less than 5–10 ppmv in the temperature range of 650–850 °C. The presence of stable CuCr<sub>2</sub>O<sub>4</sub> in CuO–Cr<sub>2</sub>O<sub>3</sub> solids retains some copper in the Cu<sup>2+</sup> or Cu<sup>1+</sup> oxidation state, which can account for the high H<sub>2</sub>S removal efficiency. In CuO–CeO<sub>2</sub> sorbents, however, CuO is easily reduced to copper metal. Participation of reduced cerium oxide in sulfidation can explain the observed high desulfurization efficiency. TGA tests and XRD analysis indicate that sulfidation proceeds through partial initial reduction of the CuO–Cr<sub>2</sub>O<sub>3</sub> sorbents: CuO → Cu/Cu<sub>2</sub>O → Cu<sub>x</sub>S (*x* < 2). Reduction kinetics were studied in the TGA over temperature ranges of 550–850 and 350–850 °C, respectively, for the CuO–Cr<sub>2</sub>O<sub>3</sub> and CuO–CeO<sub>2</sub> materials. The sulfidation kinetic parameters were measured in the temperature range of 450–850 °C after prereduction of both sorbents. The sulfidation of metal copper in Cr<sub>2</sub>O<sub>3</sub> and CeO<sub>2–x</sub> matrices is a fast reaction with low activation energy, 19.8 and 16.6 kJ/mol, respectively. Both types of sorbents can be fully regenerated with diluted air. The regeneration temperature affects the reaction pathway and the regenerability of the solid composition.

## Introduction

High-temperature, regenerative desulfurization of fuel gases is under development to improve the thermal efficiency of advanced coal-based power generation systems, such as integrated gasification combined-cycle (IGCC) power plants. One of the crucial factors for the successful application of the high-temperature desulfurization technology is the development of sorbents which can effectively remove sulfur compounds, mainly H<sub>2</sub>S, from fuel gases in the temperature range of 600–800 °C. The search for sorbents with high H<sub>2</sub>S removal efficiency, good sulfur-loading capacity, high regenerability, and sufficient strength has continued unabated since the early 1980s. Early studies of single metal oxides, such as Fe<sub>2</sub>O<sub>3</sub> and ZnO, were soon followed by the development of mixed metal oxides to increase the H<sub>2</sub>S removal efficiency and regenerability of the sorbent. The mixed-oxide sorbent zinc ferrite, ZnFe<sub>2</sub>O<sub>4</sub>, combining ZnO and Fe<sub>2</sub>O<sub>3</sub> has been developed as an improvement over each of its component oxides, primary in the work performed at the Department of Energy [1,2]. Zinc ferrite, however, is prone to reduction of both its component oxides at high temperatures. Work at the Massachusetts Institute of Technology in the middle and late 1980s established zinc titanates as improved ZnO-based sorbents that could also impart stability to ZnO against reduction to elemental zinc. Formation of the latter is followed by zinc migration and/or evaporation, which cause undesired structural modifications of the sorbent in highly reducing coal gas streams [3–9]. Because of their higher stability, zinc titanates lean-in-zinc may be used at higher desulfurization temperature than ZnO or ZnFe<sub>2</sub>O<sub>4</sub> [6].

In parallel with the development of ZnO-based sorbents, other sorbent studies have been conducted with various mixed metal oxides, predominantly based on copper oxide, which can be used at much higher temperature than ZnO [4,10–16]. The low vapor pressure of copper oxides and copper metal ensures operation without volatilization. Among all metal oxides, copper oxides (CuO and Cu<sub>2</sub>O) have the highest sulfidation equilibrium constants; for example, at *T* = 900 K, *K*<sub>s</sub> =

$6.3 \times 10^{17}$  and  $8.9 \times 10^8$ , respectively, for CuO and Cu<sub>2</sub>O [17] sulfidation according to the reactions:



Thus, copper oxides can reduce H<sub>2</sub>S from several thousand ppm to sub-ppm levels. However, CuO in uncombined form is readily reduced to metallic copper by the H<sub>2</sub> and CO contained in fuel gases [13,15]. The reduction of Cu<sup>2+</sup> or Cu<sup>1+</sup> to metallic Cu lowers the desulfurization efficiency, since the sulfidation equilibrium constant of CuO is about 10 orders of magnitude higher than that of Cu. Metallic copper has an inferior desulfurization efficiency to ZnO. Another disadvantage of uncombined copper oxide is its low utilization in sulfidation caused by sintering of onion-like dense sulfide layers which dramatically increase the solid diffusion resistance and cause structural degradation of the pellet [18]. To improve the performance of CuO-based sorbents, research has focused on two approaches: (i) to maintain part of copper at the +2 or +1 oxidation state during sulfidation and (ii) to provide CuO in highly dispersed form to reduce the diffusion resistance.

In order to retain copper at the +2 or +1 oxidation state, copper oxides have been combined with other metal oxides, forming metal oxide compounds [4,10,11,14,15,18,19]. Flytzani-Stephanopoulos *et al.* [4,10] and Patrick *et al.* [14,15] studied various bulk CuO-based sorbent systems, such as Cu–Fe–O, Cu–Al–O, Cu–Fe–Al–O, and Cu–Mo–Al–O. In metal oxide compounds, such as CuFe<sub>2</sub>O<sub>4</sub> or CuAl<sub>2</sub>O<sub>4</sub>, the reduction of CuO to Cu by H<sub>2</sub> or CO was much slower than that of pure CuO. This is due both to the thermodynamic stability of these spinels and to slow kinetics. The slow reduction of CuO in these mixtures retained a portion of copper in +2 and/or +1 oxidation state and, therefore, achieved sub-ppm H<sub>2</sub>S breakthrough levels at temperatures as high as 650–700 °C depending on the fuel gas composition. Even higher

stability is provided to CuO by combining it with chromium oxide. Thus,  $\text{CuCr}_2\text{O}_4$  was found to possess the best thermodynamic stability and slowest reduction kinetics among all oxide compounds of copper [17,19].

Dispersed CuO-containing sorbents can generally be synthesized by carrying copper oxides on a support at low temperatures. For high-temperature application, however, the choice of support is crucial. Alumina, for example, will react with copper, forming stable copper aluminate phases at high temperature ( $\geq 600^\circ\text{C}$ ) either during calcination or during the sorbent regeneration step. Compound formation prevents good dispersion. Kyotani *et al.* [12,13] have compared the performance of bulk CuO with several mixed CuO materials, including physical mixtures of CuO and  $\text{SiO}_2$ , CuO dispersed in a  $\text{SiO}_2$  matrix, and CuO supported on a zeolite. They found that when dispersed CuO sorbents were used in fixed-bed reactor tests, the  $\text{H}_2\text{S}$  prebreakthrough concentration in the exit gas was reduced to lower levels than what would be predicted by the equilibrium of the reaction of metallic Cu with  $\text{H}_2\text{S}$ .  $\text{SiO}_2$  or the zeolite served as a dispersant, preventing the aggregation of CuO particles. Moreover, based on the fact that the physical mixture of CuO and  $\text{SiO}_2$  had a reactivity similar to that of the  $\text{SiO}_2$ - or zeolite-supported CuO at  $600^\circ\text{C}$ , Kyotani *et al.* [13] concluded that very high dispersion of CuO is not critical.

In recent work, we have found that the binary oxides of  $\text{CuO-Cr}_2\text{O}_3$  and  $\text{CuO-CeO}_2$  show excellent  $\text{H}_2\text{S}$  removal efficiency and high reactivity in both sulfidation and regeneration [19]. The  $\text{H}_2\text{S}$  removal efficiency of both types of sorbents was better than 99%, and complete CuO conversion was attained at  $750^\circ\text{C}$ . While, as mentioned above, Cu-Cr-O sorbents are expected to retain oxidic copper in reductive sulfidation, the opposite is true for the system  $\text{CuO-CeO}_2$ . In fact, CuO and  $\text{CeO}_2$  are totally immiscible.  $\text{CeO}_2$  is an excellent dispersant of copper and has been reported to keep a fraction of copper in cluster form (3–5 nm) even at high copper loadings [20]. It is interesting to compare the reactivities of these two very different CuO-based sorbents. In this paper we report on comparative kinetic and parametric studies of reduction, sulfidation, and regeneration conducted with bulk Cu-Cr-O and Cu-Ce-O sorbents.

## Experimental Section

**Sorbent Preparation.** The binary oxides Cu-Cr-O and Cu-Ce-O sorbents were prepared in bulk form from amorphous citrate precursors according to a method developed by Marcilly *et al.* [21]. Briefly, the preparation of bulk powders was as follows: an aqueous solution of cerium or chromium nitrate was mixed with a copper nitrate solution in the desired molar ratio. The mixed solution was then added dropwise into an aqueous solution of citric acid under continuous stirring at room temperature. Typically, a molar ratio of 1:1 of citric acid to total metals was used. The final solution was dehydrated rapidly (15–30 min) in a rotary evaporator at  $65\text{--}75^\circ\text{C}$  under vacuum to a viscous liquid endpoint, followed by slow dehydration (4–6 h) in a vacuum oven at  $70\text{--}80^\circ\text{C}$  to form a porous solid foam. The foam was then calcined in air in a muffle furnace at  $1000^\circ\text{C}$  for 1 h. After calcination, the solid was crushed and sieved to the desired size. Three sorbent compositions with  $\text{CuO:CeO}_2$  or  $\text{CuO:Cr}_2\text{O}_3$  mole ratios of 3:1, 1:1, and 1:3 were prepared for each of the Cu-Ce-O and Cu-Cr-O sorbents.

**Sorbent Characterization.** Several bulk and surface analysis methods were employed to characterize the fresh and sulfided samples. Surface area was measured by a Micromeritics Flow-Sorb II 2300 BET apparatus using  $\text{N}_2$  desorption. X-ray diffraction (XRD) for identification of crystalline phases in the sorbents was performed in a Rigaku RU300 instrument using  $\text{Cu K}\alpha$  radiation. A Cambridge Stereoscan 250 MK3 scanning electron microscope (SEM) equipped with an energy-dispersive X-ray (EDS) analyzer was used to follow the surface morphology and composition of selected samples.

**Thermobalance Reactor Tests.** The weight change of the sample during reduction, sulfidation, and regeneration was measured in a Cahn System 113-X thermogravimetric analyzer (TGA), comprising a Cahn 2000 microbalance, a Micricon temperature controller, and a data acquisition system. The inlet gas flow rate was controlled by four Brooks Model 5850 mass flow controllers. Water was injected into the heated gas line by a calibrated syringe pump. A simulated coal gas mixture containing  $\text{H}_2\text{S-H}_2\text{-H}_2\text{O-N}_2$  was used in sulfidation. Regeneration was carried out by air diluted with  $\text{N}_2$ . The total gas flow rate was 564 sccm. Reaction rates measured at various flow rates (200–600 sccm) confirmed that bulk gas diffusion limitations were eliminated at this flow rate.

In all TGA tests 2–3 mg of sorbent was placed in a hemispherical quartz pan suspended by a quartz hang-down wire. A thin layer of quartz wool was used to partially fill the quartz pan. The typical size of solid particles used was 125–180  $\mu\text{m}$ . After loading the sample, the furnace was heated to a set point at a rate of  $22^\circ\text{C}/\text{min}$  under pure  $\text{N}_2$  and was maintained at the set value throughout the experiment. Typically, reduction lasted for 10 min, sulfidation for 20 min, and regeneration for 10 min. An intermittent nitrogen purge for 20 min was used between sulfidation and regeneration tests.

**Packed-Bed Microreactor Tests.** Sulfidation and regeneration tests were performed in a packed-bed microreactor to evaluate the overall  $\text{H}_2\text{S}$  removal efficiency and regenerability of the synthesized sorbents. The packed-bed microreactor system and experimental procedure were the same as those previously described by Lew *et al.* [5–8]. About 50 mg of sorbent of 420–800  $\mu\text{m}$  in diameter was used. Dry gas mixtures containing  $\text{H}_2\text{S-H}_2\text{-N}_2$  were used to screen the sorbents. The gas hourly space velocity, SV, was  $3000\text{ h}^{-1}$  (NTP).  $\text{H}_2\text{S}$  and  $\text{SO}_2$  concentrations in the exit gas were measured by a HP 5880A gas chromatograph (GC), equipped with a flame photometric detector (FPD) and a thermal conductivity detector (TCD) used respectively during sulfidation and regeneration.

## Results and Discussion

**Characterization of Fresh Sorbents.** Table 1 lists the physical properties of fresh binary Cu-Cr-O and Cu-Ce-O sorbents prepared in this work. At a calcination temperature of  $1000^\circ\text{C}$ , the specific surface area of the two types of sorbents decreased with the CuO content. X-ray diffraction identified that cupric chromite,  $\text{CuCr}_2\text{O}_4$ , was formed in the CuO-lean Cu-Cr-O sorbent, while the excess chromium oxide was in the form of  $\text{Cr}_2\text{O}_3$ . For the equimolar  $\text{CuO-Cr}_2\text{O}_3$  material,  $\text{CuCr}_2\text{O}_4$  was the only crystalline phase formed and no separate CuO or  $\text{Cr}_2\text{O}_3$  phases were identified. Cuprous chromite,  $\text{CuCrO}_2$ , and CuO phases coexisted in the CuO-rich sorbent,  $3\text{CuO-Cr}_2\text{O}_3$ . For Cu-Ce-O sor-

**Table 1. Characterization of Fresh and Sulfided Sorbents**

sorbent	BET surface area <sup>a</sup> (m <sup>2</sup> /g)	max. theoretical sulfur loading <sup>b</sup> (g of sulfur/100 g of sorbent)	crystalline phases <sup>c</sup>	
			fresh	sulfided <sup>d</sup>
3CuO–Cr <sub>2</sub> O <sub>3</sub>	0.6	12.2	CuCrO <sub>2</sub> , CuO	Cr <sub>2</sub> O <sub>3</sub> , Cu <sub>9</sub> S <sub>5</sub> , Cu <sub>2</sub> O
CuO–Cr <sub>2</sub> O <sub>3</sub>	2.2	6.7	CuCr <sub>2</sub> O <sub>4</sub>	Cr <sub>2</sub> O <sub>3</sub> , Cu <sub>9</sub> S <sub>5</sub>
CuO–3Cr <sub>2</sub> O <sub>3</sub>	3.7	3.0	CuCr <sub>2</sub> O <sub>4</sub> , Cr <sub>2</sub> O <sub>3</sub>	Cr <sub>2</sub> O <sub>3</sub> , Cu <sub>9</sub> S <sub>5</sub>
3CuO–CeO <sub>2</sub>	1.1	17.7	CuO, CeO <sub>2</sub>	CeO <sub>2</sub> , Cu <sub>8</sub> S <sub>5</sub> , Ce <sub>2</sub> S <sub>3</sub>
CuO–CeO <sub>2</sub>	4.4	6.4	CuO, CeO <sub>2</sub>	CeO <sub>2</sub> , Cu <sub>8</sub> S <sub>5</sub> , Ce <sub>2</sub> S <sub>3</sub>
CuO–3CeO <sub>2</sub>	5.8	2.7	CuO, CeO <sub>2</sub>	CeO <sub>2</sub> , Cu <sub>8</sub> S <sub>5</sub> , Cu <sub>1.8</sub> S, Ce <sub>2</sub> S <sub>3</sub>

<sup>a</sup> After calcination in air at 1000 °C for 1 h. <sup>b</sup> Assuming Cu<sub>2</sub>S as the only sulfidation product. <sup>c</sup> Identified by X-ray diffraction analysis. <sup>d</sup> Sulfided under 2% H<sub>2</sub>S–20% H<sub>2</sub>–78% N<sub>2</sub> at 850 °C.

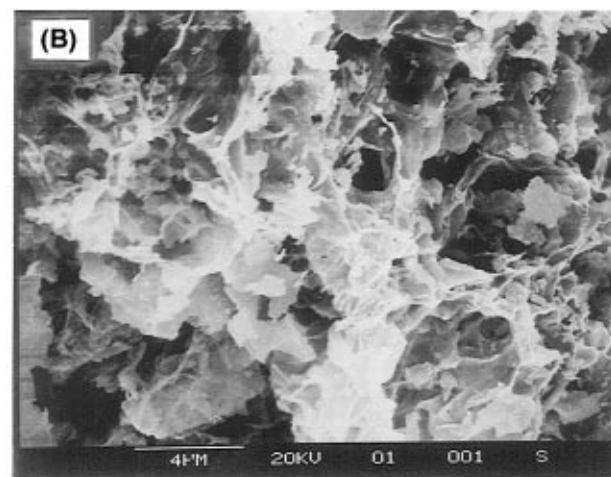
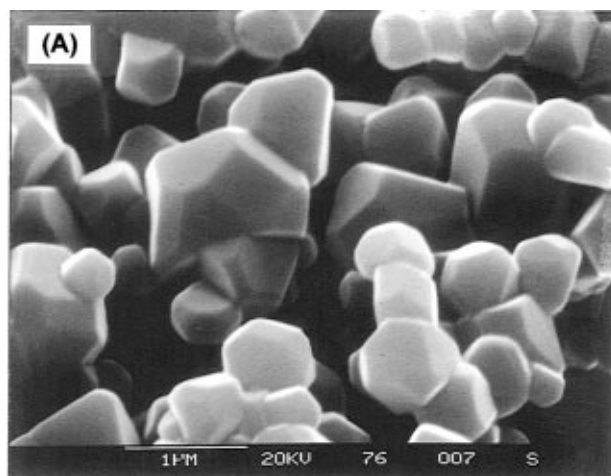


**Figure 1.** SEM of fresh solid samples: (A) CuO–Cr<sub>2</sub>O<sub>3</sub>, calcined at 1000 °C for 1 h, 21 000×; (B) CuO–CeO<sub>2</sub>, calcined at 1000 °C for 1 h, 5000×.

bents, the XRD data in Table 1 show that no compounds were formed for all three Cu–Ce–O sorbents. CuO and CeO<sub>2</sub> existed in separate phases in all sorbent compositions.

Parts A and B of Figure 1 show scanning electron micrographs of the fresh equimolar CuO–Cr<sub>2</sub>O<sub>3</sub> and CuO–CeO<sub>2</sub> sorbents. As can be seen from Figure 1A, well-formed CuCr<sub>2</sub>O<sub>4</sub> crystals were produced after calcination at 1000 °C. These crystals have a uniform size of ~0.5 μm. Figure 1B shows a very different structure for the CuO–CeO<sub>2</sub> sorbent. No separate phase of CuO could be discerned on ceria by SEM. By the use of high-resolution scanning transmission electron microscopy and EDS, however, Liu *et al.*, have identified CuO particles and clusters in Cu–Ce–O materials [20].

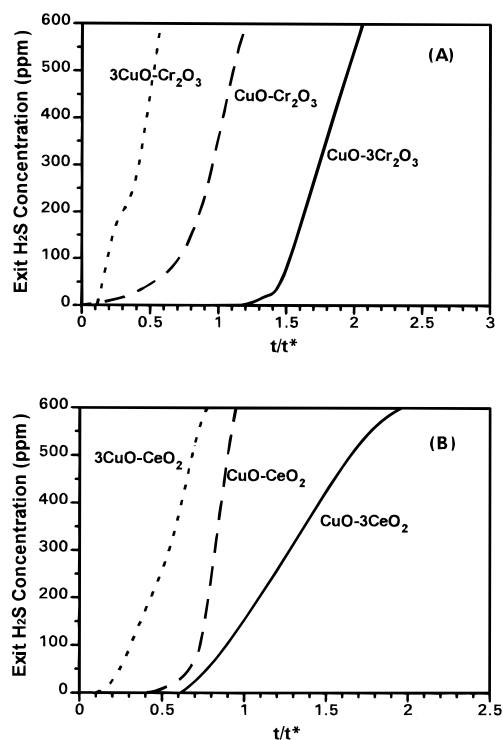


**Figure 2.** H<sub>2</sub>S breakthrough curves for (A) Cu–Cr–O and (B) Cu–Ce–O sorbents with various CuO/Cr<sub>2</sub>O<sub>3</sub> or CuO/CeO<sub>2</sub> ratios. Sulfidation conditions:  $T = 850$  °C, inlet gas 2% H<sub>2</sub>S–20% H<sub>2</sub>–78% N<sub>2</sub>, SV = 3000 h<sup>-1</sup> (NTP).

More experiments were conducted for CuO-rich and CuO-lean Cu–Cr–O and Cu–Ce–O sorbents. The crystals in 3CuO–Cr<sub>2</sub>O<sub>3</sub> and CuO–3Cr<sub>2</sub>O<sub>3</sub> solids were not as uniform as those in equimolar samples, and the average crystal sizes were ~2 and ~0.3 μm, respectively. The 3CuO–CeO<sub>2</sub> and CuO–3CeO<sub>2</sub> samples had structures similar to that of the CuO–CeO<sub>2</sub> sorbent.

**Sulfidation of the Cu–Cr–O and Cu–Ce–O Solids. Packed-Bed Microreactor Tests.** Sulfidation tests were performed in the packed-bed microreactor with each of the six Cu–Cr–O and Cu–Ce–O sorbent compositions listed in Table 1. A gas mixture containing (mol) 2% H<sub>2</sub>S–20% H<sub>2</sub>–78% N<sub>2</sub> at SV = 3000 h<sup>-1</sup> (NTP) was used in these tests. The resulting performance is shown in Figure 2 in terms of H<sub>2</sub>S breakthrough curves at 850 °C. The normalized time,  $t/t^*$ , is defined as the ratio of the real reaction time,  $t$ , to the theoretical time,  $t^*$ , required for complete sulfidation of the amount of sorbent used in each test to form Cu<sub>2</sub>S. Thus,  $t/t^*$  corresponds to active sorbent conversion. This assumes that neither Cr<sub>2</sub>O<sub>3</sub> nor CeO<sub>2</sub> forms bulk sulfides under the tested conditions. It also assumes the absence of nonstoichiometric sulfides of copper. The H<sub>2</sub>S breakthrough time is reported here for 100 ppmv H<sub>2</sub>S in the effluent gas.

The H<sub>2</sub>S breakthrough curves in Figure 2 show that complete desulfurization of the feed gas stream can be obtained for all the Cu–Cr–O and Cu–Ce–O sorbents even at the high temperature of 850 °C. The conversion of copper at breakthrough was higher in the Cu-lean sorbents, CuO–3Cr<sub>2</sub>O<sub>3</sub> and CuO–3CeO<sub>2</sub>. As the CuO content was increased, H<sub>2</sub>S breakthrough occurred earlier, with corresponding lower CuO utilization. For example, the normalized prebreakthrough time decreased from 1.5 to 0.65 to 0.2 as the CuO/Cr<sub>2</sub>O<sub>3</sub> molar ratios changed from 1/3 to 1/1 to 3/1, respectively. A plausible explanation for this is that, in higher CuO-containing sorbents, CuO exists in larger crystals, which provide increased diffusion resistance to the reactant gas through a shell of product Cu<sub>2</sub>S. Assuming the Cu<sub>2</sub>S stoichiometry, the calculated sulfur loading of the sorbents at 100 ppmv H<sub>2</sub>S breakthrough level was approximately 2.2, 3.7, and 4.3 g of sulfur per 100 g of sorbent for the 3CuO–Cr<sub>2</sub>O<sub>3</sub>, CuO–Cr<sub>2</sub>O<sub>3</sub>, and CuO–3Cr<sub>2</sub>O<sub>3</sub> sorbents and 4.4, 4.2, and 2.2 g of sulfur per 100 g of sorbent for the 3CuO–CeO<sub>2</sub>, CuO–CeO<sub>2</sub> and CuO–3CeO<sub>2</sub> sorbents, respectively. Compared to the theoretical values listed in Table 1, the actual utilization of copper in Cu-rich sorbents is very low. On the other hand, in Cu-lean sorbents full utilization of copper has been achieved. Interestingly, the actual sulfur loading exceeds the theoretical value for the CuO–3Cr<sub>2</sub>O<sub>3</sub> sorbent (see also Figure 2A). As discussed below, this may be due to formation of nonstoichiometric sulfides.

Figure 2 shows prebreakthrough levels of H<sub>2</sub>S (<5 ppm) that are much lower than the equilibrium H<sub>2</sub>S levels corresponding to reaction of metallic copper with H<sub>2</sub>S, i.e., 2Cu + H<sub>2</sub>S = Cu<sub>2</sub>S + H<sub>2</sub>. Under the conditions of these experiments (850 °C, 20% H<sub>2</sub>), the equilibrium H<sub>2</sub>S level is ~300 ppmv [17]. Hence, the active sorbent phase is not copper metal under these conditions. Similar observations were made with other gas compositions and temperatures both in this lab and in bench-scale reactor tests conducted at the Institute of Gas Technology using the equimolar CuO–Cr<sub>2</sub>O<sub>3</sub> and CuO–CeO<sub>2</sub> sorbents [22]. The presence of various amounts of hydrogen, water vapor, and carbon oxides in the reactant gas does not affect the H<sub>2</sub>S prebreakthrough level, although it can shift the breakthrough time [19,22].

**Characterization of Sulfided Solids.** Sulfided solids from the packed-bed microreactor tests were analyzed by XRD and SEM. As shown in Table 1, Cu<sub>9</sub>S<sub>5</sub> is the major phase of copper sulfides for all three Cu–Cr–O compositions after sulfidation. Cr<sub>2</sub>O<sub>3</sub> was also identified by XRD, while no chromium sulfides were found. A small amount of Cu<sub>2</sub>O (based on signal intensity) was observed for the sulfided 3CuO–Cr<sub>2</sub>O<sub>3</sub> solid, in agreement with the low Cu utilization of this sorbent composition in the microreactor test. For the Cu–Ce–O mixtures, Cu<sub>8</sub>S<sub>5</sub> was the major sulfide phase. Also, CeO<sub>2</sub> appeared to have reacted with H<sub>2</sub>S to form cerium sulfides, since Ce<sub>2</sub>S<sub>3</sub> was consistently identified by XRD in the sulfided Cu–Ce–O sorbents. This is in agreement with the report that reduced cerium oxides, CeO<sub>2-x</sub>, are good sulfidation materials at high temperatures [23]. In regards to Figure 2, it is not accurate to estimate  $t^*$  on the basis of only Cu<sub>2</sub>S formation. However, even if approximate, the normalized time used in Figure 2 provides a measure of sorbent conversion. In practice, a more meaningful measure is that of sulfur loading, which can be used as the abscissa when comparing H<sub>2</sub>S breakthrough profiles [22].

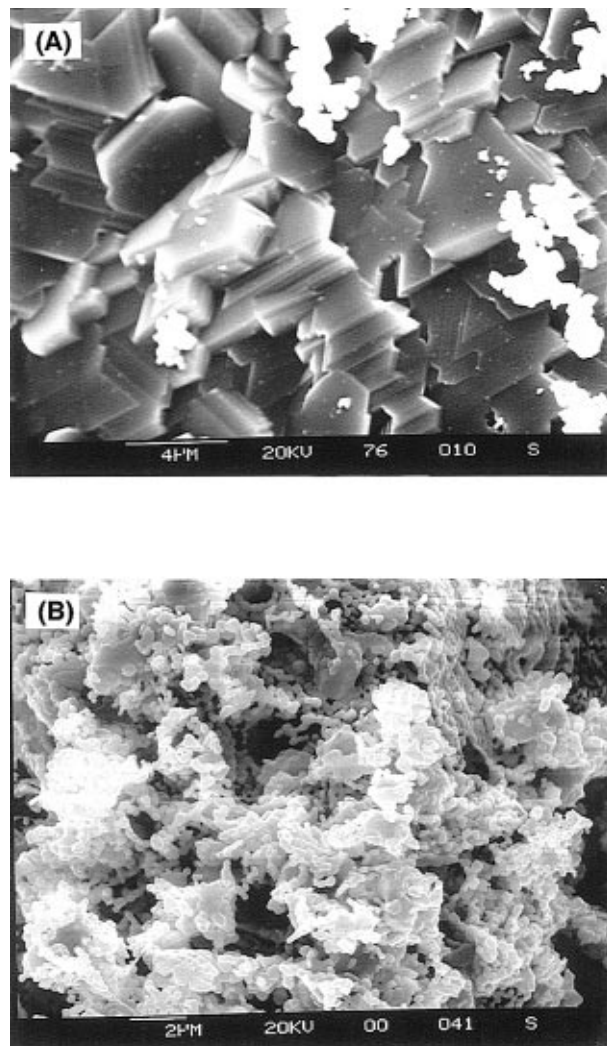


**Figure 3.** SEM of sulfided solid samples: (A) CuO–Cr<sub>2</sub>O<sub>3</sub>, 4600×; (B) CuO–CeO<sub>2</sub>, 5000×. Both samples were sulfided at 850 °C with 2% H<sub>2</sub>S–20% H<sub>2</sub>–bal N<sub>2</sub>.

SEM pictures of the fully sulfided sorbents are shown in parts A and B of Figure 3 for the equimolar CuO–Cr<sub>2</sub>O<sub>3</sub> and CuO–CeO<sub>2</sub>, respectively. The sulfidation was performed with 2% H<sub>2</sub>S–20% H<sub>2</sub>–78% N<sub>2</sub> gas mixture at 850 °C and SV = 3000 h<sup>-1</sup>. Figure 3A shows that sulfided CuO–Cr<sub>2</sub>O<sub>3</sub> has very different crystal structure from the fresh solid in Figure 1A, due to the different phases: CuCr<sub>2</sub>O<sub>4</sub> in the fresh vs Cr<sub>2</sub>O<sub>3</sub> and Cu<sub>9</sub>S<sub>5</sub> in the used sorbent. Compared with the microstructure of the fresh CuO–CeO<sub>2</sub> sorbent in Figure 1B, small crystals of ~0.4 μm in diameter were formed after sulfidation of the CuO–CeO<sub>2</sub> material, as shown in Figure 3B.

**Thermobalance Reactor Tests.** Further tests were conducted with the equimolar sorbents, CuO–Cr<sub>2</sub>O<sub>3</sub> and CuO–CeO<sub>2</sub>, in the TGA apparatus. Figure 4 shows the weight profiles, normalized by initial sorbent weight  $W_0$ , vs reaction time during sulfidation of the fresh CuO–Cr<sub>2</sub>O<sub>3</sub> and CuO–CeO<sub>2</sub> sorbents at 650, 750, and 850 °C in a gas mixture containing (mol) 0.5% H<sub>2</sub>S–10% H<sub>2</sub>–10% H<sub>2</sub>O–bal N<sub>2</sub>. It should be noted that, due to the particular stoichiometry of 2CuO → Cu<sub>2</sub>S, the final (fully sulfided) sorbent weight will be equal to the weight of the unsulfided sorbent. From Figure 4 it is apparent that the weight change during sulfidation consists of two segments: an initial weight loss followed by weight gain. Such weight change behavior points to two reactions taking place during reductive sulfidation: one

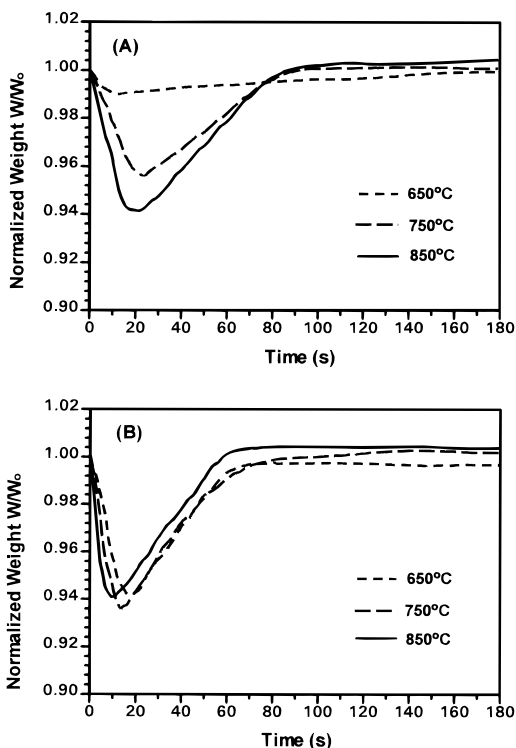


**Figure 4.** Normalized sorbent weight profiles during sulfidation of (A) CuO-Cr<sub>2</sub>O<sub>3</sub> and (B) CuO-CeO<sub>2</sub> at various temperatures. Sulfidation conditions: feed gas 0.5% H<sub>2</sub>S-10% H<sub>2</sub>-10% H<sub>2</sub>O-bal N<sub>2</sub>.

is the reduction of Cu<sup>2+</sup> oxides to Cu<sup>1+</sup> oxides or metal copper, with concomitant weight decrease; the second is sulfidation of metal copper or copper oxides to copper sulfides, leading to weight increase. Although both reduction and sulfidation reactions occurred simultaneously once the sorbents were contacted with the inlet gas containing H<sub>2</sub> and H<sub>2</sub>S, reduction was much faster than sulfidation and dominated the earlier part of the reaction. As the reaction proceeded, sulfidation began to dominate the entire reaction. Thus, the reaction path for sulfidation of these copper oxide-containing sorbents appears to be CuO → Cu<sub>2</sub>O/Cu → Cu<sub>x</sub>S (*x* < 2) over the tested temperature range.

Comparing parts A and B of Figure 4, it is seen that the reduction of CuO-Cr<sub>2</sub>O<sub>3</sub> sorbent was much slower when the temperature was decreased from 850 to 650 °C. However, temperature had little effect on the CuO-CeO<sub>2</sub> sorbent. In other words, reduction of CuO-CeO<sub>2</sub> took place to the same extent at all temperatures in the range of 650-850 °C. For the CuO-Cr<sub>2</sub>O<sub>3</sub> sorbent consisting of CuCr<sub>2</sub>O<sub>4</sub> compound, the stability of CuCr<sub>2</sub>O<sub>4</sub> suppresses reduction, especially at *T* ≤ 750 °C. This can explain why the H<sub>2</sub>S removal efficiency obtained in the packed-bed microreactor was higher than that of copper metal (Figure 2A). On the other hand, the reducibility of the Cu-Ce-O sorbents shown in Figure 4B does not match the H<sub>2</sub>S removal efficiency shown in Figure 2B. If all the copper is reduced to a metallic state, then the exit H<sub>2</sub>S level in Figure 2B should be approximately 300 ppm as stated above (based on the sulfidation equilibrium of Cu). While it may be argued that some oxidic form of copper remains in the cerium oxide matrix, it is more plausible to assume that partial reduction of cerium can account for some of the observed loss of oxygen. The reducibility of bulk ceria is greatly enhanced by the presence of CuO [24]. Reduced cerium

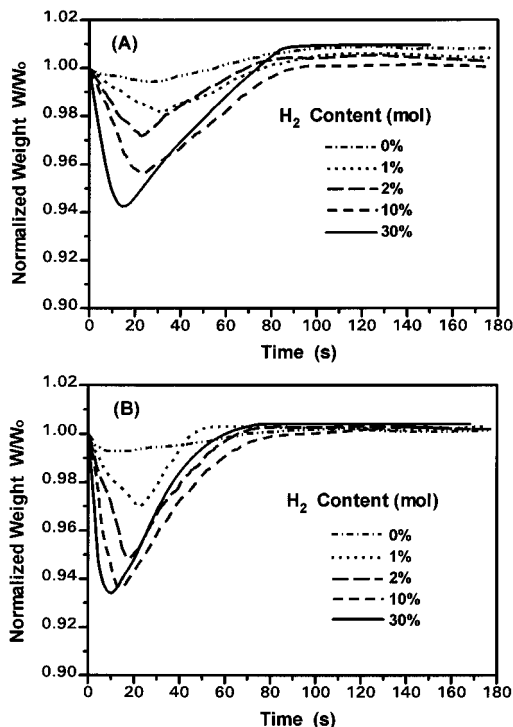


**Figure 5.** Normalized sorbent weight profiles during sulfidation of (A) CuO-Cr<sub>2</sub>O<sub>3</sub> and (B) CuO-CeO<sub>2</sub> at various H<sub>2</sub> concentrations. Sulfidation conditions: *T* = 750 °C, feed gas 0.5% H<sub>2</sub>S-*x*% H<sub>2</sub>-10% H<sub>2</sub>O-bal N<sub>2</sub>.

oxide is an excellent H<sub>2</sub>S sorbent [23]. The presence of Ce<sub>2</sub>S<sub>3</sub> in the sulfided sorbents (Table 1) corroborates this argument.

Further direct sulfidation tests of the fresh sorbent samples were conducted in the TGA under various conditions. The effect of H<sub>2</sub> concentration on sulfidation at *T* = 750 °C is shown in parts A and B of Figure 5 for CuO-Cr<sub>2</sub>O<sub>3</sub> and CuO-CeO<sub>2</sub>, respectively. For both sorbents, the reduction rate and extent of reduction increased with the H<sub>2</sub> concentration. At temperatures above 750 °C complete reduction of CuO to metallic copper during sulfidation took place for CuO-Cr<sub>2</sub>O<sub>3</sub> sorbents when H<sub>2</sub> was above 30 mol % (Figure 5A). For CuO-CeO<sub>2</sub> sorbents, a lower H<sub>2</sub> concentration of 10 mol % was sufficient to reduce the sorbent to an extent corresponding to all oxidic copper reduced to the metal state. As can be seen in Figure 5A,B, a small weight decrease was measured even when the inlet gas did not contain H<sub>2</sub> (H<sub>2</sub> = 0% curves). Two factors could contribute to the weight decrease at this condition. One is the reduction of CuO by H<sub>2</sub> produced by the decomposition of H<sub>2</sub>S, while the other is the oxidation of H<sub>2</sub>S by CuO or CeO<sub>2</sub> to form SO<sub>2</sub>. The former was verified by the condensation of elemental sulfur on the cooler walls of the quartz tube and in the water trap located downstream of the TGA. The equilibrium H<sub>2</sub> concentration for H<sub>2</sub>S decomposition at 750 °C is calculated to be ~1400 ppm in the absence of hydrogen in the inlet gas. On the other hand, the oxidation of H<sub>2</sub>S to SO<sub>2</sub> has been reported to be catalyzed by ceria [25]. To check for this, we analyzed the TGA off-gas in the GC-FPD. The measurement showed that approximately 50 ppm SO<sub>2</sub> could be obtained in the TGA outlet gas when a low H<sub>2</sub> concentration (<10 mol %) was used. Thus, under some conditions, other reactions, such as decomposition and/or oxidation of H<sub>2</sub>S, can also take place in addition to the main sulfidation reaction.

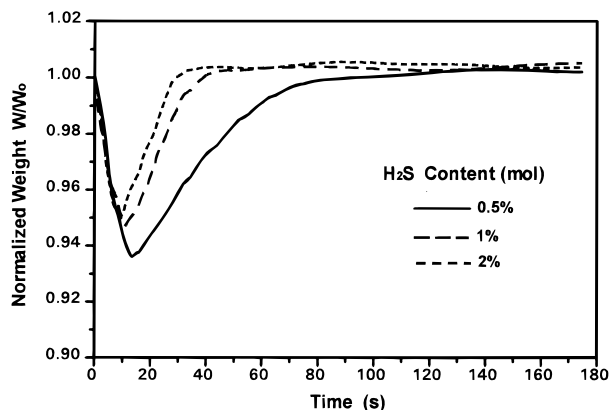


**Figure 6.** Normalized sorbent weight profiles during sulfidation of CuO–CeO<sub>2</sub> at various H<sub>2</sub>S concentrations. Sulfidation conditions:  $T = 750\text{ }^{\circ}\text{C}$ , feed gas  $x\%$  H<sub>2</sub>S–10% H<sub>2</sub>–10% H<sub>2</sub>O–bal N<sub>2</sub>.

Sulfidation of fresh sorbent samples at various H<sub>2</sub>S concentrations is shown in Figure 6 for the CuO–CeO<sub>2</sub> sorbent. Similar results were found for the CuO–Cr<sub>2</sub>O<sub>3</sub>. Increasing the H<sub>2</sub>S concentration led to faster sulfidation rate. Thus, at higher H<sub>2</sub>S concentrations fresh sorbents were less extensively reduced and showed an early weight increase. For example, at 2% H<sub>2</sub>S, the weight loss due to reduction is 77% of that observed at 0.5% H<sub>2</sub>S and the weight gain begins 5 s earlier. From Figure 6, it is also obvious that H<sub>2</sub>S has little effect on the reduction rate at 750 °C, as indicated by the overlapping of the reduction segments of the normalized weight profiles at various H<sub>2</sub>S concentrations.

**Comparative Kinetics of Reduction and Sulfidation of Cu–Cr–O and Cu–Ce–O.** To better study the above reductive sulfidation behavior, separate tests of reduction and sulfidation of prerduced sorbent samples were performed in the TGA. The kinetics of reduction of CuO–Cr<sub>2</sub>O<sub>3</sub> and CuO–CeO<sub>2</sub> were compared. Also, comparative studies of the kinetics of prerduced Cu–Cr<sub>2</sub>O<sub>3</sub> and Cu–CeO<sub>2-x</sub> materials were conducted as described below.

**Reduction Kinetics.** Reduction tests were conducted over a wide temperature range from 350 to 850 °C in a gas mixture containing (mol) 10% H<sub>2</sub>–10% H<sub>2</sub>O–80% N<sub>2</sub>. The effect of temperature on reduction is shown in Figure 7. When the temperature was decreased from 850 to 550 °C, the reduction rate of CuCr<sub>2</sub>O<sub>4</sub> decreased dramatically, (Figure 7A), but for CuO–CeO<sub>2</sub>, no appreciable change of reduction rate was found even over a wider temperature range (350–850 °C). In temperature-programmed-reduction (TPR) experiments with Cu–Ce–O, Liu et al. [24] have found a bimodal reduction by hydrogen. A 15(at)% Cu-containing cerium oxide showed a TPR profile with a first peak at 120–145 °C corresponding to CuO reduction and a broader second peak from 450 to 850 °C corresponding to CeO<sub>2</sub> reduction. Notably, each phase alone is less reducible.

Reduction of the CuO–Cr<sub>2</sub>O<sub>3</sub> and CuO–CeO<sub>2</sub> solids under various H<sub>2</sub> concentrations was conducted at 750 °C with [H<sub>2</sub>] = 2–40 mol %. Figure 8 shows the profiles of the normalized weight vs time at three H<sub>2</sub> concentrations: 2, 10, and 40%. Over the tested H<sub>2</sub> concentration range, the reduction of both sorbents was rather fast at 750 °C. As can be seen from this figure, the reduction rate of both sorbents increased with the H<sub>2</sub> concentration in the feed stream. The CuO–Cr<sub>2</sub>O<sub>3</sub> material showed a stronger dependence on H<sub>2</sub> concentration than CuO–CeO<sub>2</sub>, apparently due to the stability of the CuCr<sub>2</sub>O<sub>4</sub> compound.

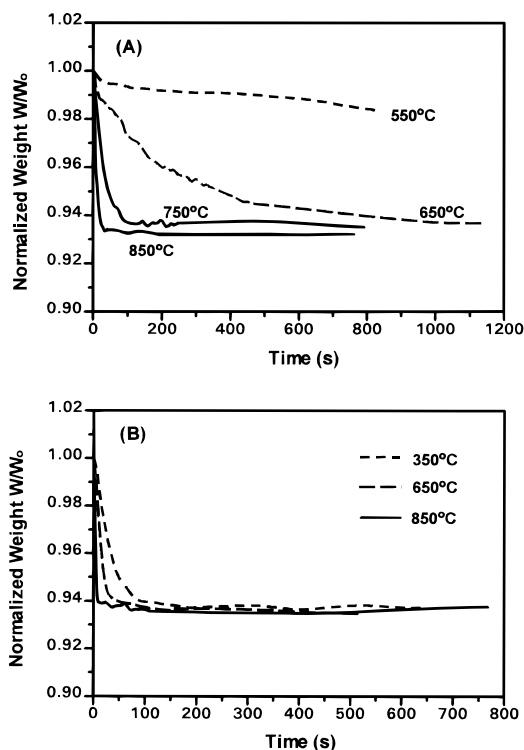


**Figure 7.** Normalized sorbent weight profiles during reduction of (A) CuO–Cr<sub>2</sub>O<sub>3</sub> and (B) CuO–CeO<sub>2</sub> at various temperatures. Reduction conditions: feed gas 10% H<sub>2</sub>–10% H<sub>2</sub>O–bal N<sub>2</sub>.

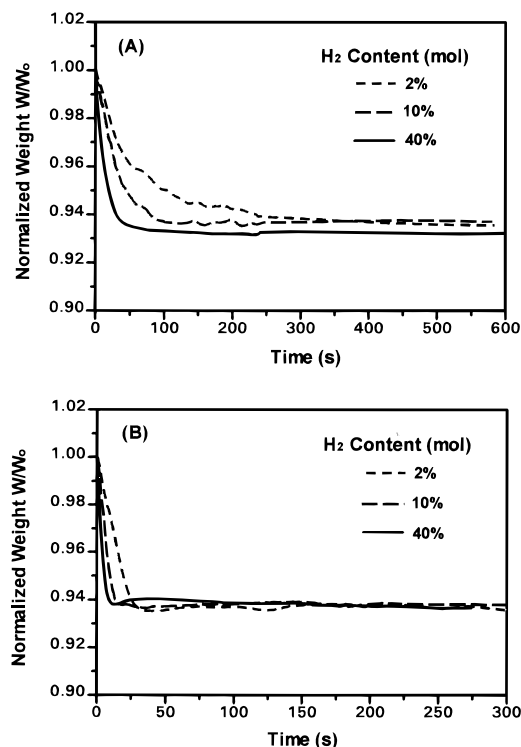


**Figure 8.** Normalized sorbent weight profiles during reduction of (A) CuO–Cr<sub>2</sub>O<sub>3</sub> and (B) CuO–CeO<sub>2</sub> at various H<sub>2</sub> concentrations. Reduction conditions:  $T = 750\text{ }^{\circ}\text{C}$ , feed gas  $x\%$  H<sub>2</sub>–10% H<sub>2</sub>O–bal N<sub>2</sub>.

Initial reduction rates were measured from the slopes of the  $W/W_0$  profiles in Figures 7 and 8 at time  $t = 0$ . The initial reduction rates,  $R_0$ , can be expressed as surface rates of reduction of CuO, by dividing the slope  $d(W/W_0)/dt$  at  $t = 0$  by the surface area of the sorbent,  $A_0$  (m<sup>2</sup>/g), and by the molecular weight of the escaping species, considering the reaction stoichiometry. Here,

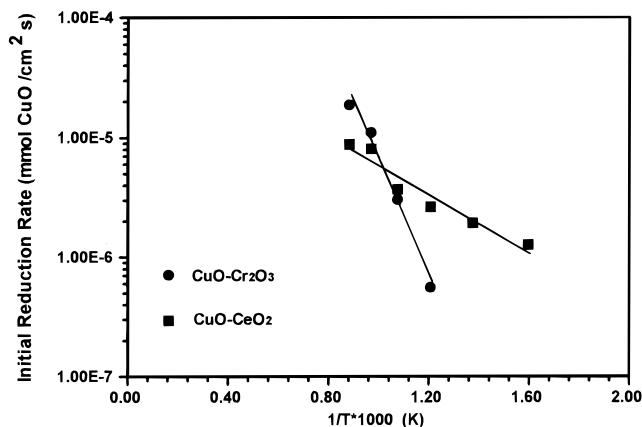


**Figure 9.** Arrhenius-type plot of initial reduction rate vs temperature for CuO-Cr<sub>2</sub>O<sub>3</sub> and CuO-CeO<sub>2</sub>. Feed gas: 10% H<sub>2</sub>-10% H<sub>2</sub>O-80% N<sub>2</sub>.

this is  $1/2$  mol of oxygen for each 1 mol of CuO. In calculating the initial reduction rates for CuO-CeO<sub>2</sub>, we assumed that CuO was the faster of the two oxides. Figure 9 shows Arrhenius-type plots for the initial reduction rates of CuO-Cr<sub>2</sub>O<sub>3</sub> and CuO-CeO<sub>2</sub>. The rates, expressed in mmol of CuO·cm<sup>-2</sup>·s<sup>-1</sup>, were measured over the temperature range of 550–850 °C. The reaction order in H<sub>2</sub>,  $n$ , was determined to be 0.58 and 0.42, respectively, for CuO-Cr<sub>2</sub>O<sub>3</sub> and CuO-CeO<sub>2</sub> at 750 °C. Assuming constancy of this order with temperature, reaction rate constants can be calculated using the expression  $R_0 = k_r C_{H_2}^n$ . Table 2 lists the values of the Arrhenius constants  $k_{r,0}$  and  $E_a$  for the reduction rate constants expressed in Arrhenius form:  $k_r = k_{r,0} \times \exp(-E_a/RT)$ , for each of the two CuO-based sorbents.

From Figure 8, it is seen that at 750 °C the surface reduction kinetics (initial reduction rates) prevail also at large sorbent conversions in the presence of more than 10 mol % H<sub>2</sub> in the feed gas. However, under different conditions, the rate may become limited by gas diffusion through the solid. This is particularly so for the CuO-Cr<sub>2</sub>O<sub>3</sub> sorbent, which is limited by diffusion at 750 °C when the hydrogen level is 2 or 10%, as shown in Figure 8A by the lower slope of the  $W/W_0$ -time curves at long times.

**Sulfidation of Prereduced Sorbents.** Sulfidation of reduced sorbents was conducted at 650, 750, and 850 °C by first reducing the sample at a fixed condition, i.e., at 750 °C with a gas mixture containing (mol) 10% H<sub>2</sub>-10% H<sub>2</sub>O-80% N<sub>2</sub>, and then introducing the sulfidation gas mixture containing (mol) 10% H<sub>2</sub>-10% H<sub>2</sub>O-0.5% H<sub>2</sub>S-bal N<sub>2</sub>. As an example, Figure 10 shows the sulfidation of prereduced Cu-Cr<sub>2</sub>O<sub>3</sub> at various temperatures. Similar profiles were obtained for Cu-CeO<sub>2-x</sub>. As a result of complete prereduction, sulfidation of Cu in both samples was fast and almost independent of temperature in the range of 650–850 °C. Complete conversion of Cu to copper sulfides was achieved at all conditions tested except at 650 °C for Cu-Cr<sub>2</sub>O<sub>3</sub> as shown in Figure 10, where the final normalized weight was slightly less than 1. From several comparisons of the overall kinetics at 750 and 850 °C, the Cu-CeO<sub>2-x</sub> material appeared to have faster sulfidation. This difference may be caused by the different pore structure of the two sorbents and the potential participation of cerium oxide in sulfidation of the prereduced Cu-CeO<sub>2-x</sub> material.

Parts A and B of Figure 11 show sulfidation profiles of prereduced Cu-Cr<sub>2</sub>O<sub>3</sub> and Cu-CeO<sub>2-x</sub> samples,

respectively, at various concentrations of H<sub>2</sub>S. Clearly, the rates increase appreciably with the H<sub>2</sub>S concentration. With the exception of the Cu-Cr<sub>2</sub>O<sub>3</sub> at 0.125% H<sub>2</sub>S (Figure 11A), the  $W/W_0$  increased linearly with the reaction time up to complete conversion, indicating that sulfidation rates were not limited by diffusion at 750 °C.

Initial rates of sulfidation of prereduced sorbents were obtained from the slopes of  $W/W_0$ -time profiles at  $t = 0$  in Figures 10 and 11 and other similar data. The stoichiometry of the sulfidation of metallic copper was assumed:  $2Cu + H_2S = Cu_2S + H_2$ , and the BET surface area of the prereduced solids was used to calculate the initial rate,  $R_0$ , in terms of moles of Cu<sub>2</sub>S produced per unit time per unit area (Table 2). Figure 12 shows the Arrhenius-type plots of the initial sulfidation rates for Cu-Cr<sub>2</sub>O<sub>3</sub> and Cu-CeO<sub>2-x</sub>. The reaction order in H<sub>2</sub>S,  $n$ , at 750 °C was 0.70 for the former and 0.83 for the latter. Assuming constancy of these orders with temperature, the sulfidation rate constant can be calculated for  $R_0 = k_s C_{H_2S}^n$ . Table 2 shows the Arrhenius constants  $k_{s,0}$  and  $E_a$  for  $k_s = k_{s,0} \exp(-E_a/RT)$ . The activation energies of copper metal sulfidation are much lower than the corresponding values for the reduction of the precursor oxides. Thus, sulfidation is a weak function of temperature. This finding is in agreement with sulfidation kinetics of other metals, e.g., iron in a matrix of silica [26] or the oxides of zinc, manganese, and calcium [8,27]. The most plausible explanation for these very low activation energies is that of H<sub>2</sub>S adsorption limitation [26,28].

While there is a difference between the initial rates of sulfidation of Cu-CeO<sub>2-x</sub> and Cu-Cr<sub>2</sub>O<sub>3</sub>, the difference is not large (Figure 12). This is anticipated if the reactive phase in both prereduced materials is metallic copper. In terms of fast intrinsic sulfidation kinetics, MnO and Cu metal are ranked the best, followed by ZnO, CaO, and Fe [28]. However, the overall reactivity of sorbents is the important parameter. Structural changes that may hinder regenerability and good cyclic performance often manifest themselves in reductive sulfidation of both single oxide sorbents as well as nonoptimized mixed oxides. Such is the case of ZnO-rich sorbents, as has been reported in the literature [6,8].

**Regeneration Performance.** Regeneration tests of sulfided CuO-Cr<sub>2</sub>O<sub>3</sub> and CuO-CeO<sub>2</sub> were conducted with 6 mol % O<sub>2</sub> in nitrogen over the temperature range of 650–850 °C. The results are shown in parts A and B of Figure 13 for CuO-Cr<sub>2</sub>O<sub>3</sub> and CuO-CeO<sub>2</sub>, respectively, with the initial  $W/W_0$  being slightly higher than 1 for the CuO-Cr<sub>2</sub>O<sub>3</sub> as a result of sulfidation. All samples had been sulfided completely prior to regeneration under the same conditions, as indicated in the figure.

For the CuO-Cr<sub>2</sub>O<sub>3</sub> sorbent in Figure 13A, a sharp weight decrease at the beginning of the regeneration was observed at all four temperatures, as shown in the inset of the figure. This weight loss was probably caused by the formation of intermediate Cu<sub>2</sub>O. At the lower tested temperatures of 650 and 700 °C, the weight increased very rapidly following the initial weight drop and reached a maximum in each run, probably due to the formation of CuSO<sub>4</sub>. After that the weight decreased gradually as the copper sulfate decomposed, but for the regeneration at 650 °C it did not go back to the

**Table 2. Kinetic Parameters of Sorbent Reduction and Sulfidation**

	reduction			sulfidation <sup>a</sup>		
	$k_{r,0}$ (mmol <sup>1-n</sup> cm <sup>3n-2</sup> s <sup>-1</sup> )	$E_a$ (kJ mol <sup>-1</sup> )	$n^b$	$k_{s,0}$ (mmol <sup>1-n</sup> cm <sup>3n-2</sup> s <sup>-1</sup> )	$E_a$ (kJ mol <sup>-1</sup> )	$n^b$
CuO-Cr <sub>2</sub> O <sub>3</sub>	$1.07 \times 10^3$	96.8	0.58	$2.73 \times 10^{-2}$	19.8	0.70
CuO-CeO <sub>2</sub>	$2.58 \times 10^{-2}$	26.2	0.42	$7.50 \times 10^{-2}$	16.6	0.83

<sup>a</sup> Samples used in sulfidation were prereduced at 750 °C with 10% H<sub>2</sub>-10% H<sub>2</sub>O-80% N<sub>2</sub>. The BET surface area of the prereduced sorbents was 7.43 and 4.98 m<sup>2</sup>/g, respectively, for Cu-Cr<sub>2</sub>O<sub>3</sub> and Cu-CeO<sub>2-x</sub>. <sup>b</sup> Reduction and sulfidation order in H<sub>2</sub> and H<sub>2</sub>S, respectively, from measurements at 750 °C.

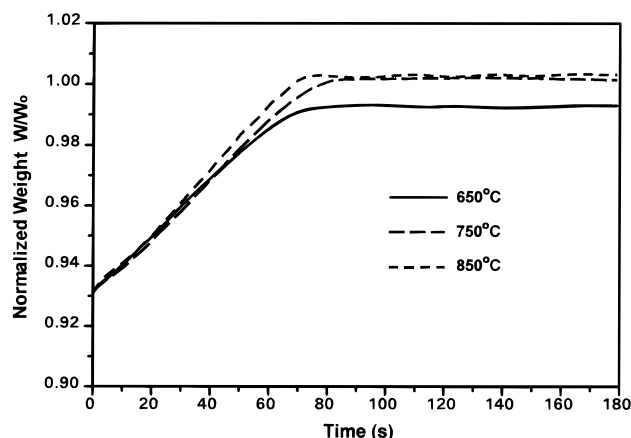


**Figure 10.** Normalized sorbent weight profiles during sulfidation of prereduced Cu-Cr<sub>2</sub>O<sub>3</sub> at various temperatures. Prereduction conditions:  $T = 750$  °C, feed gas 10% H<sub>2</sub>-10% H<sub>2</sub>O-bal N<sub>2</sub>. Sulfidation conditions: feed gas 0.5% H<sub>2</sub>S-10% H<sub>2</sub>-10% H<sub>2</sub>O-bal N<sub>2</sub>.

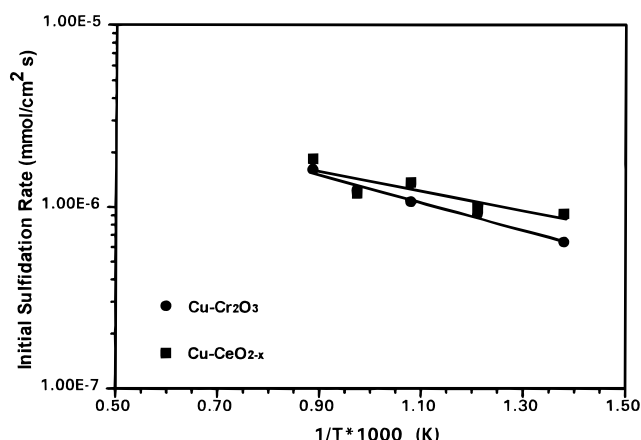


**Figure 12.** Arrhenius-type plot of initial sulfidation rate vs temperature for prereduced Cu-Cr<sub>2</sub>O<sub>3</sub> and Cu-CeO<sub>2</sub>. Feed gas: 0.5% H<sub>2</sub>S-10% H<sub>2</sub>-10% H<sub>2</sub>O-bal N<sub>2</sub>.

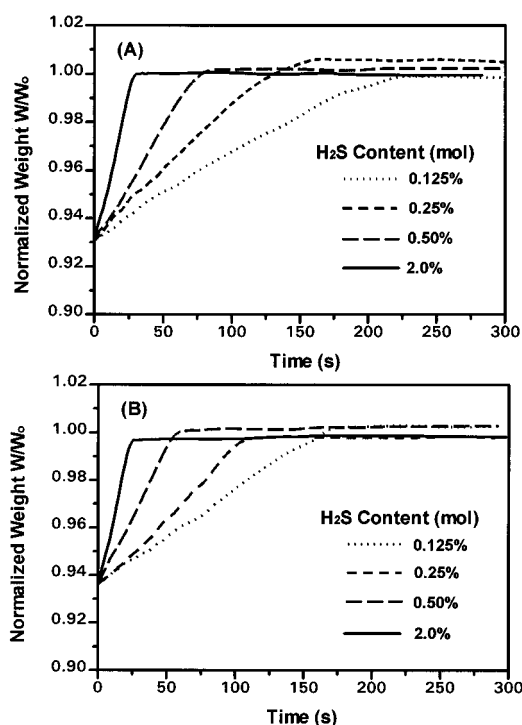


**Figure 11.** Normalized sorbent weight profiles during sulfidation of prereduced (A) Cu-Cr<sub>2</sub>O<sub>3</sub> and (B) Cu-CeO<sub>2</sub> at various H<sub>2</sub>S concentrations. Prereduction conditions:  $T = 750$  °C, feed gas 10% H<sub>2</sub>-10% H<sub>2</sub>O-bal N<sub>2</sub>. Sulfidation conditions:  $T = 750$  °C, feed gas  $x\%$  H<sub>2</sub>S-10% H<sub>2</sub>-10% H<sub>2</sub>O-bal N<sub>2</sub>.

initial value after 20 min of regeneration. The most plausible regeneration path at low temperature, therefore, is  $\text{Cu}_x\text{S} \rightarrow \text{Cu}_2\text{O}/\text{CuO} \rightarrow \text{CuSO}_4/\text{CuO} \rightarrow \text{CuO}$ . At the high temperature of 750 and 850 °C, although the weight also increased after a quick drop, it did not exceed 1 and was almost constant after it reached that

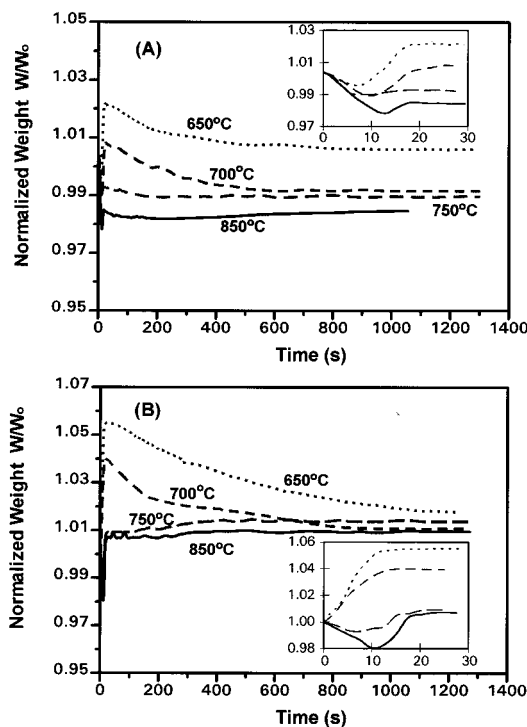


**Figure 13.** Normalized sorbent weight profiles during regeneration of sulfided (A) CuO-Cr<sub>2</sub>O<sub>3</sub> and (B) CuO-CeO<sub>2</sub> at various temperatures. Sulfidation conditions:  $T = 750$  °C, feed gas 0.5% H<sub>2</sub>S-10% H<sub>2</sub>-10% H<sub>2</sub>O-bal N<sub>2</sub>. Regeneration gas: 6% O<sub>2</sub>-94% N<sub>2</sub>.

value, implying that direct regeneration  $\text{Cu}_2\text{S} \rightarrow \text{Cu}_2\text{O}/\text{CuO}$ , i.e., without sulfate formation, took place.

Compared with the CuO-Cr<sub>2</sub>O<sub>3</sub> sorbent, different observations were made during regeneration of the CuO-CeO<sub>2</sub> sorbent, as shown in Figure 13B. A weight decrease at the beginning of regeneration was measured only at temperatures above 750 °C. At 650 and 700 °C, an immediate weight increase was observed, which was different from the case of CuO-Cr<sub>2</sub>O<sub>3</sub> at the same

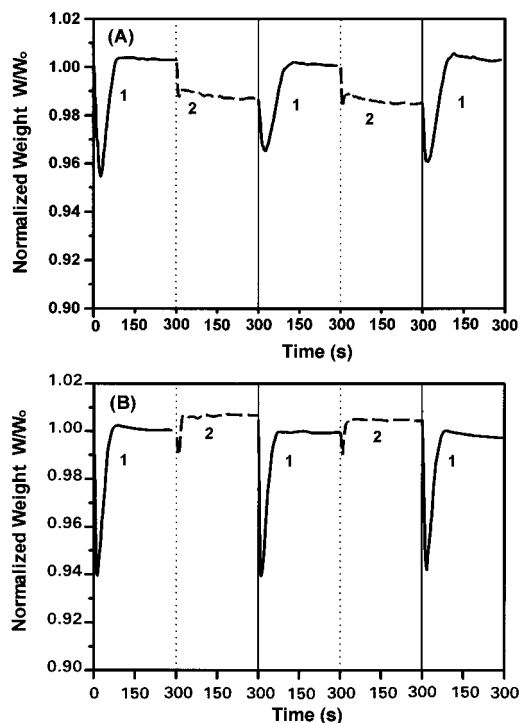


**Figure 14.** TGA sulfidation (1)–regeneration (2) cycles of (A)  $\text{CuO-Cr}_2\text{O}_3$  and (B)  $\text{CuO-CeO}_2$ . Sulfidation conditions:  $T = 750$  °C, feed gas 0.5%  $\text{H}_2\text{S}$ –10%  $\text{H}_2$ –10%  $\text{H}_2\text{O}$ –bal  $\text{N}_2$ . Regeneration conditions:  $T = 750$  °C, feed gas 6%  $\text{O}_2$ –bal  $\text{N}_2$ .

temperatures. For the  $\text{CuO-CeO}_2$  sorbent, the final normalized weights were higher than 1 after 20 min of regeneration at all tested temperatures, including 750 and 850 °C. This means that the  $\text{CuO-CeO}_2$  solid forms more stable surface sulfates than the  $\text{CuO-Cr}_2\text{O}_3$  system. This is attributed to cerium sulfate rather than  $\text{CuSO}_4$  [24].

**Multicycle Tests.** From a practical viewpoint, the  $\text{Cu-Cr-O}$  and  $\text{Cu-Ce-O}$  sorbents should possess regenerability in cyclic operation. This was shown to be good in microreactor tests. In this work, to determine the sorbent regenerability, two and a half cycles of consecutive sulfidation–regeneration were performed with the  $\text{CuO-Cr}_2\text{O}_3$  and  $\text{CuO-CeO}_2$  sorbents. The results are shown in parts A and B of Figure 14, respectively. Sulfidation was carried out with a wet gas mixture containing (mol) 0.5%  $\text{H}_2\text{S}$ –10%  $\text{H}_2\text{O}$ –10%  $\text{H}_2$ –bal  $\text{N}_2$  for 20 min. Sulfided solids were purged in nitrogen for 10 min and then regenerated with a 6 mol %  $\text{O}_2$ – $\text{N}_2$  mixture for 10 min. All reactions were performed at 750 °C. Since there was no significant weight change in the later period of sulfidation and regeneration, only the first 5 min in each of the processes are shown in Figure 14. As can be seen from this figure, no significant changes were found except the lower starting values of  $W/W_0$  for  $\text{CuO-Cr}_2\text{O}_3$  sorbent in the second and third cycles as a result of the formation of  $\text{Cu}_2\text{O}$  in the regeneration step of the previous cycles. Thus, the activities of both  $\text{CuO-Cr}_2\text{O}_3$  and  $\text{CuO-CeO}_2$  are stable in cyclic operation.

## Summary/Conclusions

$\text{CuO}$ -based sorbents were compared in this work in terms of their desulfurization efficiency and reactivity for  $\text{H}_2\text{S}$  removal from coal gas streams by high temperatures (650–850 °C). Two very different sorbent structures were selected for study. In one,  $\text{CuO-Cr}_2\text{O}_3$ , the

stable compound of copper chromite is formed, while the second,  $\text{CuO-CeO}_2$ , keeps copper in a dispersed state.  $\text{CeO}_2$  and  $\text{CuO}$  are immiscible oxides. Copper chromite has the lowest reducibility of all copper oxide-containing compounds reported in the literature. On the contrary, in the  $\text{CuO-CeO}_2$  system, the reducibility of both the  $\text{CuO}$  and  $\text{CeO}_2$  phases is enhanced.

Sulfidation tests carried out in a packed-bed microreactor have shown that equimolar  $\text{CuO-Cr}_2\text{O}_3$  and  $\text{CuO-CeO}_2$  sorbents can remove  $\text{H}_2\text{S}$  in a fuel gas to less than 5–10 ppm in the temperature range of 650–850 °C and in the presence of 20 mol %  $\text{H}_2$ –10 mol %  $\text{H}_2\text{O}$ . This is well below the equilibrium  $\text{H}_2\text{S}$  level corresponding to sulfidation of metallic copper. The presence of stable  $\text{CuCr}_2\text{O}_4$  in the  $\text{CuO-Cr}_2\text{O}_3$  solids is believed to preserve copper in the  $\text{Cu}^{2+}$  or  $\text{Cu}^{1+}$  oxidation state and, therefore, to account for the high  $\text{H}_2\text{S}$  removal efficiency. However, a similar argument cannot be made for the  $\text{CuO-CeO}_2$  sorbent, which is easy to reduce. Here the participation of reduced cerium oxide,  $\text{CeO}_{2-x}$ , in the sulfidation is invoked to explain the observed desulfurization efficiency.

In direct sulfidation of the two sorbents, in a TGA apparatus, we found that reduction and sulfidation were competing reactions. TGA tests and XRD solid analysis have indicated that sulfidation proceeds through partial initial reduction:  $\text{CuO} \rightarrow \text{Cu/Cu}_2\text{O} \rightarrow \text{Cu}_x\text{S}$  ( $x < 2$ ) for the  $\text{CuO-Cr}_2\text{O}_3$  sorbents. The extent of reduction depends on temperature and feed gas composition as well as the solid composition. The  $\text{CuO-CeO}_2$  sorbent was reduced appreciably even with low  $\text{H}_2$  gas concentrations.

Comparative kinetics of reduction and sulfidation of prereduced sorbents were conducted in the TGA under conditions free of mass-transfer limitations. The activation energy for reduction of the two sorbents is very different, i.e., 96.8 and 26.2 kJ/mol for  $\text{CuO-Cr}_2\text{O}_3$  and  $\text{CuO-CeO}_2$ , respectively. The activation energy for sulfidation is very low, 19.8 and 16.5 kJ/mol, for prereduced  $\text{Cu-Cr}_2\text{O}_3$  and  $\text{Cu-CeO}_{2-x}$ , respectively, indicating that the reaction may be adsorption limited.

In regeneration the reaction paths were complex over the tested temperature range. At low temperatures, intermediate sulfate formation is suggested by the data and the reaction path appears to be  $\text{Cu}_x\text{S} \rightarrow \text{Cu}_2\text{O} \rightarrow \text{CuSO}_4/\text{CuO} \rightarrow \text{CuO}$  for  $\text{CuO-Cr}_2\text{O}_3$  and  $\text{Cu}_2\text{S} \rightarrow \text{CuSO}_4/\text{CuO} \rightarrow \text{CuO}$  for  $\text{CuO-CeO}_2$ . At higher temperature a rather simple mechanism involving no intermediate sulfate is inferred from the data for  $\text{CuO-Cr}_2\text{O}_3$ :  $\text{Cu}_2\text{S} \rightarrow \text{Cu}_2\text{O} \rightarrow \text{CuO}$ . However, in the case of  $\text{CuO-CeO}_2$ , some sulfate still persists after regeneration at 750 °C with 6%  $\text{O}_2$  in  $\text{N}_2$ . This is attributed to stable surface sulfates of cerium.

Overall, in this work we have shown that  $\text{CuO}$ -based sorbents of the type  $\text{CuO-Cr}_2\text{O}_3$  and  $\text{CuO-CeO}_2$  can be tailored to meet a wide range of applications in hot coal-gas desulfurization. Thus, the desulfurization efficiency and reactivity as well as the regenerability of the sorbent can all be optimized for a particular fuel gas composition–temperature–reactor design by suitable sorbent composition and structure selection.

## Acknowledgment

We thank Ms. Luhong Bo and Ms. Li Li for assisting with the packed-bed microreactor tests and the SEM analyses. Financial support by the Illinois Clean Coal Institute and the U.S. Department of Energy through a contract to the Institute of Gas Technology/Contract

No. DE-FC22-92PC92521, subcontract to Tufts University, is gratefully acknowledged.

### Literature Cited

- (1) Grindley, T.; Steinfeld, G. Development and Testing of Regenerable Hot Coal Gas Desulfurization Sorbents. Final Report to DOE, No. DOE/MC/16545-1125, Oct 1981.
- (2) Grindley, T.; Steinfeld, G. Zinc Ferrite as Hydrogen Sulfide Absorbent. 3rd Annual Contractors' Meeting on Contaminant Control in Hot Coal-Derived Gas Streams, 1983; Report No. DOE/METC/84-6.
- (3) Lew, S. High-Temperature Regenerative H<sub>2</sub>S Removal by ZnO-TiO<sub>2</sub> System. M.S. Thesis, MIT, Cambridge, MA, 1987.
- (4) Flytzani-Stephanopoulos, M.; Gavalas, G. R.; Jothimurugesan, K.; Lew, S.; Sharma, P. K.; Bagajewicz, M. J.; Patrick, V. Detailed Studies of Novel Regenerable Sorbents for High-Temperature Coal-Gas Desulfurization. Final Report to DOE, DE-FC21-8-MC22193, Oct 1987.
- (5) Lew, S.; Jothimurugesan, K.; Flytzani-Stephanopoulos, M. *Ind. Eng. Chem. Res.* **1989**, *28*, 535-541.
- (6) Lew, S. The Reduction and Sulfidation of Zinc Titanate and Zinc Oxide Solids. Ph.D. Dissertation, MIT, Cambridge, MA, 1990.
- (7) Lew, S.; Sarofim, A. F.; Flytzani-Stephanopoulos, M. *Chem. Eng. Sci.* **1992**, *47* (6), 1421-1431.
- (8) Lew, S.; Sarofim, A. F.; Flytzani-Stephanopoulos, M. *Ind. Eng. Chem. Res.* **1992**, *31*, 1890-1899.
- (9) Lew, S.; Sarofim, A. F.; Flytzani-Stephanopoulos, M. *AIChE J.* **1992**, *38* (8), 1161-1169.
- (10) Flytzani-Stephanopoulos, M.; Gavalas, G. R.; Tamhankar, S. S.; Sharma, P. K. Novel Sorbents for High-Temperature Regenerative H<sub>2</sub>S Removal. Final Report to DOE, DOE/MC/20417-1898, Oct 1985.
- (11) Tamhankar, S. S.; Bagajewicz, M.; Gavalas, G. R.; Sharma, P. K.; Flytzani-Stephanopoulos, M. *Ind. Eng. Chem. Process Des. Dev.* **1986**, *25*, 429-437.
- (12) Kyotani, T.; Kawashima, H.; Tomita, A.; Palmer, A.; Furimsky, E. *Fuel* **1989**, *68*, 74-79.
- (13) Kyotani, T.; Kawashima, H.; Tomita, A. *Environ. Sci. Technol.* **1989**, *23* (2), 218-223.
- (14) Patrick, V.; Gavalas, G. R.; Flytzani-Stephanopoulos, M.; Jothimurugesan, K. *Ind. Eng. Chem. Res.* **1989**, *28*, 931-940.
- (15) Patrick, V.; Gavalas, G. R. *J. Am. Ceram. Soc.* **1990**, *73* (2), 358-369.
- (16) Patrick, V.; Gavalas, G. R.; Sharma, P. K. *Ind. Eng. Chem. Res.* **1993**, *32*, 519-532.
- (17) Barin, I.; Knacke, O. *Thermochemical Properties of Inorganic Substances*; Springer Verlag: New York, 1973; Barin, I.; Knacke, O.; Kubaschewski, O. *Ibid.*, Supplement, 1977.
- (18) Sick, G.; Schwerdtfeger, K. *Metall. Trans.* **1987**, *18B*, 603-609.
- (19) Abbasian, J.; Flytzani-Stephanopoulos, M.; Hill, A. H.; Bo, L.; Wangerow, J. R. Development of Novel Copper-Based Sorbents for Hot-Gas Cleanup. IGT-Final Technical Report to CRSC, IGT Project No. 40330, Aug 1992.
- (20) Liu, W.; Flytzani-Stephanopoulos, M. *J. Catal.* **1995**, *153*, 304-316, 317-332.
- (21) Marcilly, C.; Courty, P.; Delmon, B. *J. Am. Ceram. Soc.* **1970**, *53* (1), 56-57.
- (22) Abbasian, J.; Hill, A. H.; Flytzani-Stephanopoulos, M.; Li, Z. Development of Novel Copper-Based Sorbents for Hot-Gas Cleanup. IGT-Final Technical Report to ICCI/DOE, DE-FC22-92PC92521, Aug 1994.
- (23) Kay, D. A. R.; et al. U.S. Patent 4,826,664, 1989.
- (24) Liu, W.; Wadia, C.; Flytzani-Stephanopoulos, M. *Catal. Today* **1996**, *28* (4).
- (25) Cahn, R. H.; Longo, J. M. U.S. Patent 4,346,063, 1982.
- (26) Tamhankar, S. S.; Hasatani, H.; Wen, C. Y. *Chem. Eng. Sci.* **1981**, *36*, 1181-1191.
- (27) Westmoreland, P. R.; Gibson, J. B.; Harrison, D. P. *Environ. Sci. Technol.* **1977**, *91*, 488-491.
- (28) Flytzani-Stephanopoulos, M.; Li, Z. Desulfurization of Hot Coal Gas with Regenerable Metal Oxide Sorbents: New Developments. NATO-ASI Proceedings, Kusadasi, Izmir, Turkey, July 7-19, 1996.

Received for review May 6, 1996

Revised manuscript received October 9, 1996

Accepted October 22, 1996<sup>⊗</sup>

IE960245D

---

<sup>⊗</sup> Abstract published in *Advance ACS Abstracts*, December 15, 1996.